MODELING OF ROTOR BOW DURING HOT RESTART IN CENTRIFUGAL COMPRESSORS

by

Leonardo Baldassarre

Engineering Executive & Principal Engineer for Centrifugal Compressors

and

Michele Fontana

Senior Engineer for Centrifugal Compressors

General Electric Oil & Gas Company

Florence, Italy

Leonardo Baldassarre is Engineering Manager & Principal Engineer for Compressors & Expanders with General Electric Oil & Gas Company, in Florence, Italy. He is responsible for all requisition, standardization, and CAD automation activities as well as detailed design of new products for centrifugal compressors, reciprocating compressors and turboexpanders both in Florence (Nuovo Pignone), Le Creusot (Thermodyn), and Oshkosh (AC). Dr. Baldassarre began his career with General Electric Nuovo Pignone in 1997. He has worked as Design Engineer, R&D Team Leader for centrifugal compressors, Product Leader for centrifugal and axial compressors, and Requisition Manager for centrifugal compressors both for Florence and Le Creusot teams.

Dr. Baldassarre received a B.S. degree (Mechanical Engineering, 1993) and Ph.D. degree (Mechanical Engineering/Turbomachinery Fluid Dynamics, 1998) from the University of Florence. He has authored or coauthored 20+ technical papers, mostly in the area of fluid dynamic design of 3D transonic impellers, rotating stall, and rotordynamics. He presently holds four patents.

Michele Fontana is Team Leader for Centrifugal Compressor Upstream Applications with GE Oil & Gas, in Florence, Italy. He also holds the title of Senior Engineer. His responsibilities include the support to rotordynamic study of high pressure compressors, from design stage to testing and field operation.

Mr. Fontana graduated (Mechanical Engineering, 2001) from the University of Genova. He joined GE in 2004 as a Design Engineer in the Centrifugal Compressor Requisition team, after an experience as Vibration and Dynamics Specialist in the automotive sector.

ABSTRACT

Rotor bow during hot restart is a common cause of high vibrations in turbomachinery. It may occur after the shutdown of a machine operating under load, if the rotor is left cooling in standstill condition (no turning gear) with a subsequent restart of the machine performed before the end of the thermal transient.

A complete model of the phenomenon was developed, in order to predict the amplitude of rotor vibrations during hot restart. The thermal distribution across the rotor is calculated basing on fluid-dynamic theory, and is used as boundary condition for a finite element analysis (FEA) that returns the deformed shape of the rotor. Vibration amplitude during compressor restart is then calculated with the traditional tools used for rotordynamic analysis, by unbalancing the rotor according to FEA results.

The developed model has been used to simulate a real case for which experimental data were available. Calculation results showed very good agreement with experimental measures, confirming the expected features of the phenomenon, its trend with time and the effectiveness of slow roll in straightening the rotor and reducing vibration amplitude.

INTRODUCTION

After the shutdown of a compressor operating under load, the rotor in standstill condition exchanges heat with the surrounding gas through natural convection. Due to nonuniform efficiency of the thermal exchange, the rotor cooling is asymmetrical: thermal gradients develop across each shaft section, causing the differential thermal expansion that is responsible for the rotor bow. Thermal gradients are expected to start from zero just after machine shutdown, increase up to a maximum and finally decrease back to zero when complete thermal equilibrium is reached.

The basic purpose in developing a model of the above mechanism is to identify a transfer function between system description (compressor geometry, operating parameters) and expected vibrations during startup. Such a model can be used to quantify the effect of each influencing parameter on vibration levels, and thus is useful for analyzing the design of specific compressors as well as for a general study of the hot restart phenomenon.

The complete analysis is composed of a sequence of three main modules, which are described in detail in this paper:

1. Fluid-dynamic calculation of the thermal gradients across the rotor, and of their evolution in time. This analysis is based on the theoretical formulation of natural convection on a hot, horizontal cylinder surrounded by a colder fluid.

2. Structural calculation of the deformation of the rotor due to the thermal distribution resulting from step 1. It is performed by means of finite element analysis.

3. Mechanical calculation of vibrations during startup caused by the rotor deformation obtained at step 2. This activity is performed with the same rotordynamic software that is used for the lateral analysis of the compressor.

THERMAL DISTRIBUTION ACROSS SHAFT SECTION

Following the occurrence of a compressor shutdown, the rotor tends to reach thermal equilibrium with the surrounding gas. The rotor is generally hotter than the surrounding gas, and thermal exchange between rotor and gas occurs mainly through convection.

The thermal bowing of the rotor is due to its asymmetrical cooling in standstill conditions. Considering a shaft section perpendicular to rotation axis (Figure 1), points at the top and at the bottom of the section have the same temperature right after compressor shutdown and have again the same temperature when thermal equilibrium with gas is finally reached, but during the transient the temperature differential between them reaches a maximum. This happens because thermal exchange due to natural convection is more efficient on the lower side of the rotor than on the upper side, where fluid recirculates and boundary layer are thicker.

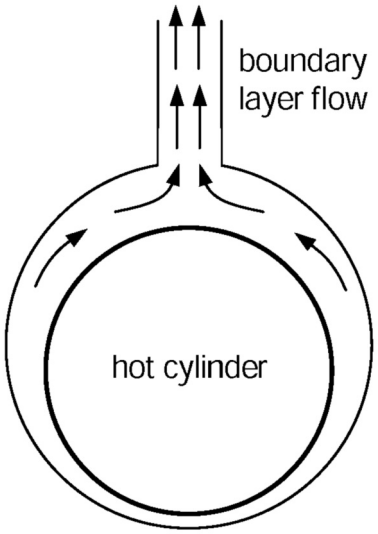

Figure 1. Schematization of Natural Convection Around Shaft Section.

The differences in temperature across the shaft section correspond to different thermal deformations of the material that cause the bending of the rotor axis. This result is an offset between the center of gravity of the bowed rotor and its bearing axis, whose effect on compressor vibrations is similar to that of an unbalance applied to the rotor.

The situation described above can be approached analytically, based on the formulation developed in fluid dynamics and heat transfer theory for the natural convection of a hot horizontal, circular cylinder surrounded by a colder fluid.

The following adimensional numbers are used:

- *Pr* = Prandtl number: ratio of viscous diffusion rate to thermal diffusion rate
- *Gr* = Grashof number: ratio of buoyancy forces to viscous forces acting on a fluid
- *Nu* = Nusselt number: ratio of convective to conductive heat transfer across a boundary between a body and a fluid

In the present case the following formulations can be assumed for these adimensional numbers (Çengel, 2003):

$$Pr = \frac{\nu}{\alpha} = \frac{c_p \mu}{\lambda} \tag{1}$$

$$Gr = \frac{g\beta(T_s - T_\infty)D^3}{\nu^2} \tag{2}$$

$$Nu = \varphi\left\{0.60 + \frac{0.387(Gr \cdot \mathrm{Pr})^{1/6}}{\left[1 + (0.559/\mathrm{Pr})^{9/16}\right]^{8/27}}\right\}^2 \tag{3}$$

Using the nomenclature below:

ν = Gas kinematic viscosity
α = Gas thermal diffusivity
μ = Gas dynamic viscosity
λ = Gas thermal conductivity
c_p = Specific heat capacity
g = Acceleration due to gravity
β = Volumetric thermal expansion coefficient, equal to approximately 1/T for ideal fluids
T_s = Source temperature
T_∞ = Asymptotic fluid temperature
D = Cylinder diameter

The factor φ in Equation (3) is a function of the angular position θ along the cylinder section (θ=0 is defined as the position at the bottom of the circle). It represents the local variation of convection efficiency, caused by the asymmetrical shape of the boundary layer sketched in Figure 1.

The function $\varphi(\theta)$ is shown in Figure 2 (refer to Oertel, 2004, for further reference). The variation of φ in function of θ results in an asymmetric thermal distribution across the section and thus in the thermal bow of the rotor, since the convective heat transfer coefficient h is related to Nu and therefore to φ:

$$h = Nu^*\lambda/D \tag{4}$$

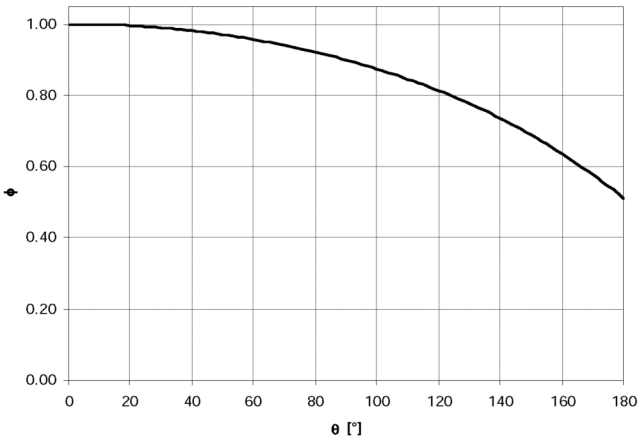

Figure 2. Relative Variation of Heat Transfer Efficiency in Function of Angular Position.

The heat transfer rate due to convection across a surface S is:

$$\frac{dQ}{dt} = hS(T_s - T_\infty) \quad (5)$$

In order to evaluate the rotor bow, the following procedure is applied:

1. The rotor section is divided in two halves (Figure 3). The factor φ is averaged over each semicircle, obtaining the two values φ_{up}=0.736 and φ_{down}=0.966.

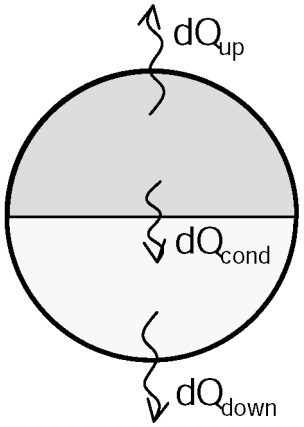

Figure 3. Shaft Section Divided in Two Half Circles. In the Time Interval dt the Heat Transferred by Convection from the Shaft to the Surrounding Gas is dQ_{up}+dQ_{down}; in Addition There Is a Heat Transfer by Conduction Between the (Warmer) Upper Half and the (Colder) Lower Half, Represented by the Term dQ_{cond}.

2. The initial values of *Pr, Gr, Nu, h,* dQ/dt are calculated for the two semicircles at t=t_0, using Equations (1) to (5) and imposing the following boundary conditions:

$$T_{s\_up}(t_0) = T_{s\_down}(t_0) = T_{s0} \quad (6)$$

T_∞ = constant function of t and θ (this simplifying assumption is justified by the small ratio between the thermal capacity of the rotor and that of the surrounding system [gas volume and compressor casing]).

3. Considering a small time interval dt, the temperatures $T_{s\_up}(t_0+dt)$ and $T_{s\_down}(t_0+dt)$ can be calculated combining the effects of convective heat transfer (between gas and rotor section) and conductive heat transfer (between upper and lower halves of the rotor section), using the formulas below:

$$T_{s\_up}(t_0+dt) = T_{s\_up}(t_0) - (dQ_{up}-dQ_{cond})/C_p \quad (7)$$

$$T_{s\_down}(t_0+dt) = T_{s\_down}(t_0) - (dQ_{down}+dQ_{cond})/C_p \quad (8)$$

$$\frac{dQ_{cond}}{dt} = \lambda_r \Delta T_s(t_0)\frac{A}{L} \quad (9)$$

C_p = Heat capacity of each half section
A = Area of contact between the two half sections
L = Average distance, can be considered approximately equal to D/2
λ_r = Thermal transmissibility of rotor material

$$\Delta T_s = T_{s\_up} - T_{s\_down} \quad (10)$$

4. The calculations described at steps 2 and 3 are repeated for a successive time interval; the values of *Gr, Nu, h,* dQ/dt are recalculated at time t=t_0+dt, updating Equations (2) to (5) with the temperature values $T_{s\_up}(t_0+dt)$ and $T_{s\_down}(t_0+dt)$ calculated above. Then the results are put into Equations (7) to (9) in order to get temperatures $T_{s\_up}(t_0+2dt)$ and $T_{s\_down}(t_0+2dt)$.

The recursive calculation described above can be applied over an arbitrarily long time span, in order to study the whole thermal transient after shutdown. The calculation is performed for each rotor section.

The resulting trends of T_{s_up}, T_{s_down} and ΔT_s depend on system geometry and initial conditions, but they are always qualitatively similar to those plotted in Figures 4 to 5. The features predicted at the beginning of this section are confirmed by diagrams: at the beginning of the thermal transient (i.e., just after compressor shutdown) the temperature difference between the top and bottom of the shaft section is zero, then it increases up to a maximum due to asymmetry in thermal exchange, and finally it decreases back to zero when complete thermal equilibrium between the rotor and the surrounding gas is reached. The highest vibrations during compressor startup will be experienced if the hot restart occurs after a time t_1 from shutdown, when ΔT_s reaches its maximum and therefore the thermal bowing of the rotor is most severe.

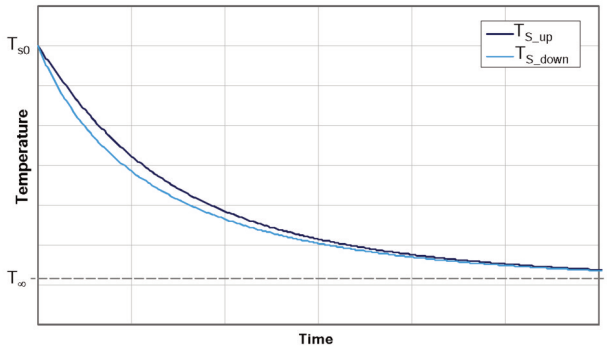

Figure 4. Average Temperature of Upper and Lower Half Shaft Section, in Function of Time.

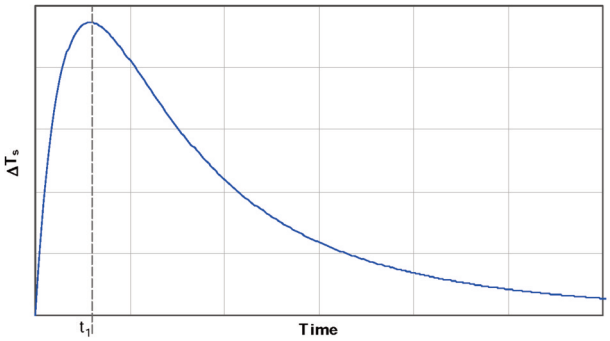

Figure 5. Difference between T_{S_up} and T_{S_down}, in Function of Time.

Simplifying Assumptions

The application of the analytical model described above to the study of hot restart in a centrifugal compressor is done under some further assumptions, in order to simplify the problem and to limit the required input data to the information that is commonly available during the design and testing of a compressor. Comparison with available experimental data shows that the error introduced by these assumptions is small enough to be acceptable for the purposes of the present analysis.

- The "cantilevered" parts of the impeller(s) and balance drum(s) are neglected from the analysis (part above the dashed line in Figure 6), since their contribution to shaft deformation is extremely small. In fact the axial length of the contact section with the shaft is very short in comparison to the bearing span, thus the bending moment and the heat flow transmitted to the shaft are negligible.

- Thermal exchange between rotor and gas is considered only in the central section of the rotor, corresponding to the gas flowpath (Figure 7). On the shaft ends it can be neglected, due to the small temperature differences between rotor, stator and gas volumes between them.

• Gas temperature and pressure after shutdown are considered uniform in each compression section.

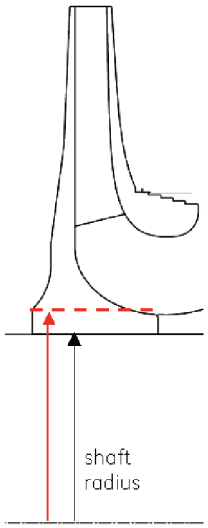

Figure 6. Equivalent Shaft Radius Considered for Calculation.

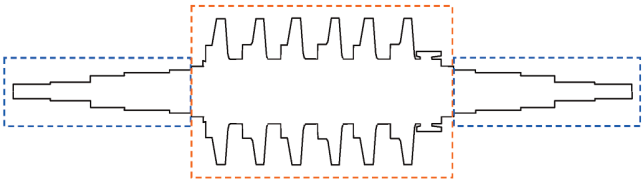

Figure 7. Rotor Schematization. Thermal Gradients Across Shaft Sections Are Calculated Only for the Center Part of the Rotor, That Is in Contact with Process Gas.

SHAFT DEFORMATION AND EFFECT ON VIBRATIONS

The deformation of the shaft due to differential thermal expansion is calculated by means of a finite element analysis, imposing as boundary conditions the temperature gradients calculated according to the procedure described in the previous section.

FEA results (Figure 8) allow evaluation of the radial displacement r_G of the center of gravity of the rotor, measured from its rotation axis (Figure 9).

Figure 8. Shaft FEA Results; Colors Represent Radial Displacement from Bearing Axis.

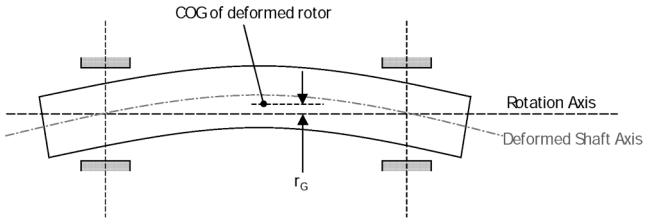

Figure 9. Rotor Bowed Due to Thermal Gradients.

The definition of rotor unbalance given by API 617, Chapter 1, paragraph 2.6.2.7 (2002) is:

$$U = 6350*W/N \quad (11)$$

where U is expressed in g·mm, N is the MCS (in rpm) and W is the weight of the rotor (in kg). The unbalance U_r produced by the offset r_G can be written in analogy to Equation (11) as:

$$U_r = W \cdot r_G \quad (12)$$

where, if kilograms and microns are used as units for W and r_G, respectively, the resulting unbalance is still expressed in g·mm as in Equation (11).

Since the deformed shape of a bowed rotor is quite similar to its first critical speed modeshape (at least if the compressor does not have overhung impellers), the rotordynamic behavior of the bowed rotor may be modeled by applying the unbalance U_r at the midspan of the undeformed rotor model (Figure 10). This approximation is acceptable for the system in study, where the effect of rotor bow on vibration amplitude measured at probes is almost completely due to the resulting unbalance, while the component due to the initial bow itself is comparatively negligible.

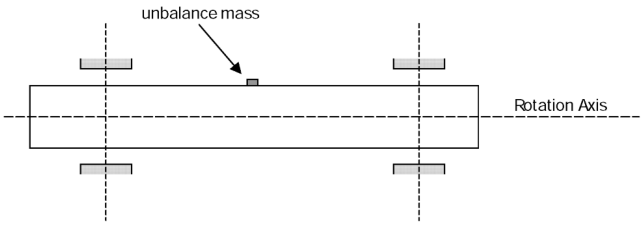

Figure 10. Straight Rotor with Unbalance Applied at Midspan: this System Is Approximately Equivalent to That of Figure 9 with Respect to Rotordynamic Behavior.

An ordinary damped unbalanced response analysis is then performed on the rotor model, in order to predict the vibrations caused by the rotor bow.

MODEL VALIDATION BY COMPARISON WITH EXPERIMENTAL DATA

Experimental Evaluation of r_G

The damped response to unbalance of a BCL358 compressor was calculated for the first critical speed according to API 617 (2002) procedure, by exciting the rotor with an unbalance 4U placed at midspan. The resulting vibration amplitude A of the first critical speed peak, calculated at the drive end (DE) and the nondrive end (NDE) radial probe locations, is equal to 11 μm and 8 μm, respectively (Figure 11).

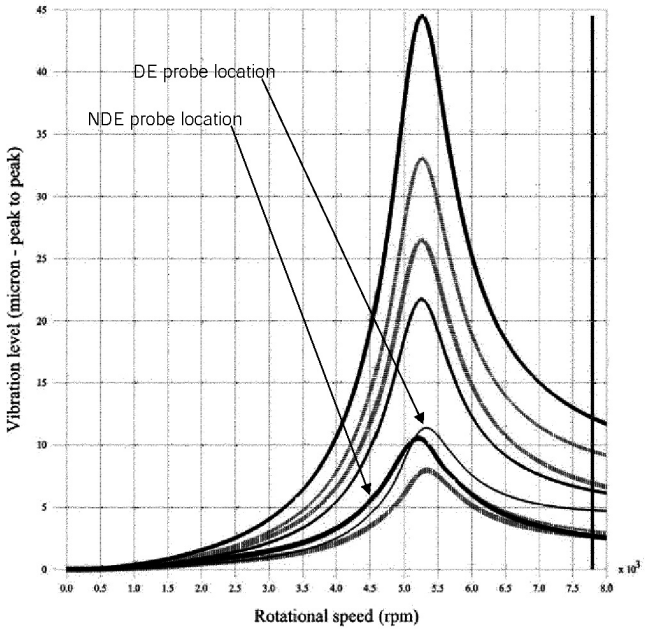

Figure 11. Calculated Vibration Amplitude (Damped Response to Unbalance).

The same BCL358 compressor experienced high vibrations due to hot restart during testing activities. The Bode diagrams of radial vibrations measured during hot restart (Figure 12) show values A_r = 64 to 88 μm of the synchronous vibration amplitude very close to first critical speed peak; the peak was expected at about 5200 rpm, but the compressor tripped due to high vibrations just before 5000 rpm. Possible values of 75 to 100 μm at peak may be inferred from the available data.

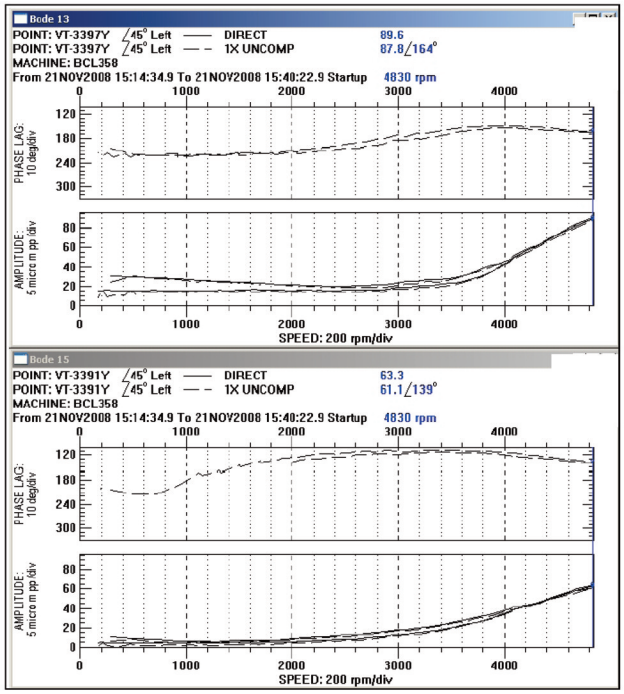

Figure 12. Measured Vibrations at Radial Probes, in Function of Speed (Bode Plots). Top Diagram Refers to Drive-End Side, Bottom Diagram Refers to Opposite Drive-End Side.

Since the relation between vibration amplitude and unbalance magnitude is linear with very good approximation in this range of values, the following relation can be written:

$$\frac{U_r}{4U} = \frac{A_r}{A} \cong 9 \tag{13}$$

where U_r is the unbalance acting on the rotor during hot restart. Therefore the displacement r_G can be calculated from Equations (11), (12) and (13), substituting the speed value of the compressor in study (N = 11692 rpm):

$$r_G = \frac{U_r}{W} = \frac{6350}{N}\frac{U_r}{U} \cong 20\,\mu m \tag{14}$$

Analytical Evaluation of r_G

The fluid dynamic model previously described was applied to the BCL358 compressor in the study, describing its geometry and conditions during hot restart with the following values to be used as initial input in Equations (1) to (8):

ν = 3.10×10^{-8} m²/s
μ = 1.31×10^{-6} Pa·s
λ = 0.036 W/mK
λ_r = 29 W/mK
c_p = 2318 J/kgK
D = 183 mm
T_s = 110°C
T_∞ = 95°C

Other parameters describing the rotor are summarized below for information:

Bearing span	1479 mm
Rotor length	1949 mm
Rotor weight	390 kg
Max. cont. speed	11692 rpm
No. of stages	8
Stage configuration	In line
Shaft diam. at journal brgs.	90 mm
Shaft diam. at impellers	163 mm

The resulting curve representing the thermal gradient ΔT as a function of time is plotted in Figure 13. The compressor was restarted after 50 minutes from shutdown, so the thermal gradient for t=50 minutes is considered in input to the FEA of the shaft model.

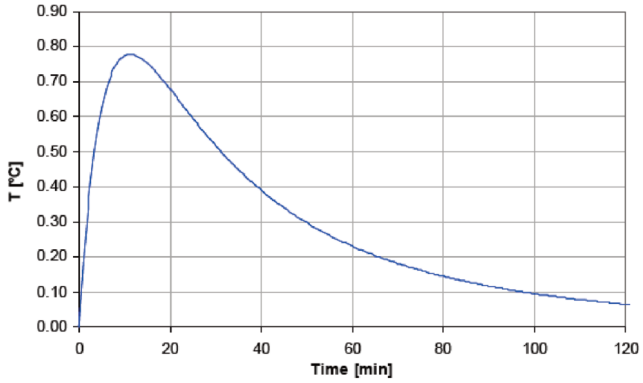

Figure 13. Thermal Gradient in Function of Standstill Duration.

FEA results can be used to quantify the rotor bow, plotting the radial displacement between the deformed shaft axis and the bearing axis (Figure 14). Since the mass distribution of the rotor along its axis is known from the geometric model, the resulting displacement r_G of the center of gravity can be calculated and is equal to 17 μm. This value is in very good agreement with the value obtained from experimental measurements reported in the section, "*Experimental Evaluation of* r_G" (20 μm).

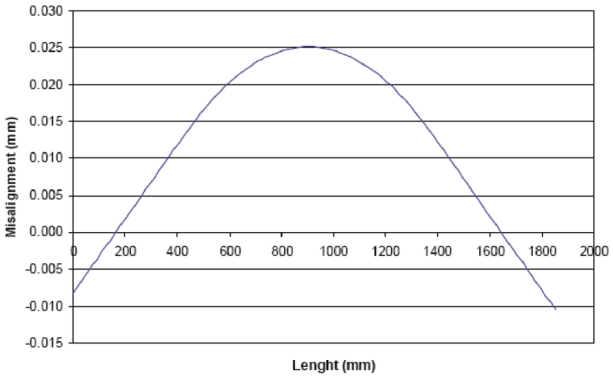

Figure 14. Analytical Evaluation of Rotor Bow.

MITIGATION OF ROTOR BOW AND FURTHER MODEL VALIDATION

In order to further validate the developed model, a specific test campaign was carried out during the testing of a 2BCL505/N centrifugal compressor (radially split casing, back-to-back arrangement, five impellers), whose vibrations during hot restart were correctly predicted by this analysis. In particular the following statements had to be verified:

- Measured vibrations were mostly due to rotor bow, therefore they should disappear if bowing is eliminated.

• Vibration amplitude is dependent on the thermal gradient ΔT across the shaft; therefore the highest vibrations should be measured if the restart occurs in proximity of the maximum of ΔT, while low amplitude is expected if the compressor is restarted just after the shutdown, or after a long standstill (ΔT close to zero in both cases).

Rotor bow is naturally eliminated during compressor rotation, since it has the effect of equalizing the shaft temperature across each section. Therefore if a compressor is subject to hot restart and then its speed is held constant, thermal gradients should gradually disappear and vibrations are expected to decrease towards an asymptotic amplitude value (that depends on residual rotor unbalance, runout and other vibration sources). This is exactly the behavior observed during test: Figure 15 displays a Bode diagram of the rotor, showing the decrease of vibrations during the 10 minute constant rotation (slow roll) at about 3400 rpm. Data measured during slow roll by the same probes are plotted in Figure 16 as a function of time, at constant speed: synchronous vibration amplitude has a decreasing (negative-exponential) trend, corresponding to the progressive elimination of rotor bow.

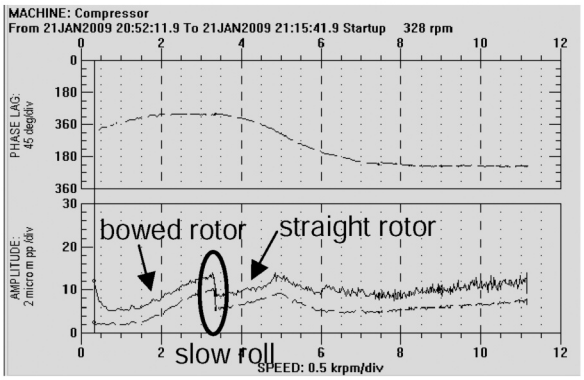

Figure 15. Bode Diagram Measured During Hot Restart Test.

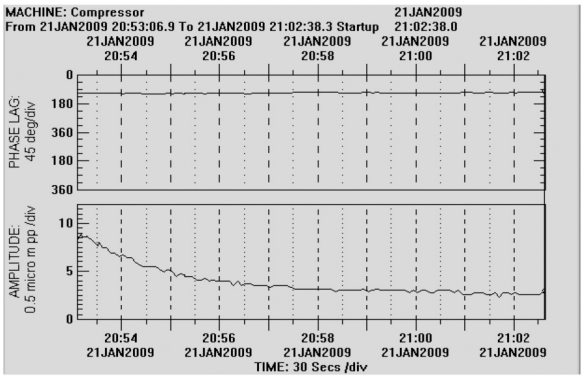

Figure 16. Compressor Vibrations in Function of Time, During Slow Roll Cycle.

Similar tests were repeated, restarting the compressor after different standstill intervals. Vibration amplitude due to rotor bow may be evaluated as the difference between vibration levels (averaged over the four probes), measured at the beginning and at the end of a slow roll cycle at 3400 rpm. This vibration amplitude is plotted in Figure 17 versus standstill duration; it may be compared with the calculated time evolution of the thermal gradient across the shaft (Figure 18) and its predicted effect on vibrations (Figure 19). The same trend can be identified between measured and calculated data, with low values for very short and very long stops and a maximum corresponding to intermediate duration of the standstill, for which thermal gradients are higher. Differences between diagrams in Figure 17 and 19 can be explained as follows:

• The maximum in the calculated curve occurs earlier than in the experimental curve; one reason is that the calculation starts from the instant at which the rotor speed is zero and the gas pressure and temperature have the same uniform value, while these conditions require some minutes to be reached starting from the commanded shutdown. This time shift can be confirmed by the shape of the curve interpolating the experimental data, whose continuation on the left side would cross the horizontal axis at t>10 mins.

• The predicted vibration amplitude is higher than the measured one. This can be explained with an attenuation of the rotor bow in experimental conditions versus the calculation model. For example the shutdown of the compressor and the ramp up to slow roll speed do not occur instantaneously; their effect is similar to slowroll itself, reducing the thermal gradients across the shaft.

Moreover, in Equation (12) the equivalent unbalance due to rotor bow has been calculated multiplying the displacement r_G by 100 percent of the rotor mass W; this is probably a conservative approach, representing the most unfavorable scenario.

Another effect that limits the vibration reduction during slow roll is described at the following point.

• The experimental curve approaches zero more quickly than the calculated curve. The main reason is that during standstill the temperature of lube oil and journal bearings also decreases. When the rotor is restarted this temperature is relatively low, then it increases during slow roll cycle; therefore the stiffness of the bearings decreases during slow roll, and consequently the vibration amplitude tends to increase. This effect is not accounted for in the calculation model that is limited to rotor bow simulation, and partially compensates the vibration reduction due to rotor straightening. The effect is that for long standstill durations (i.e., small residual rotor bow), the net difference in vibration amplitude between start and end of slow roll cycle may approach zero and even become negative.

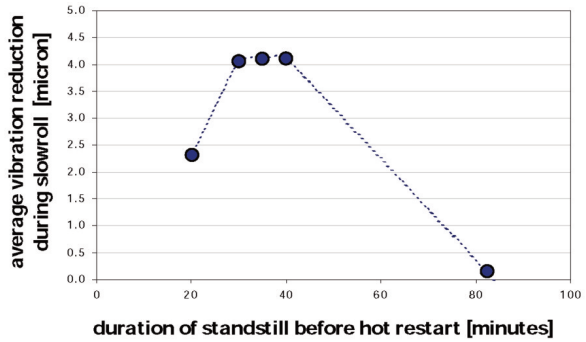

Figure 17. Indirect Measurement of Rotor Bow in Function of Standstill Duration. Rotor Bow is Proportional to the Part of Vibration Amplitude That Is Eliminated During Slow Roll.

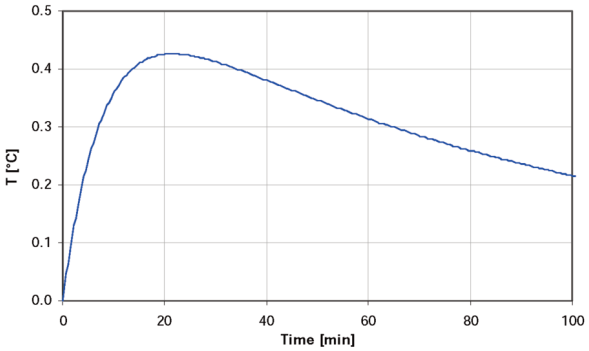

Figure 18. Predicted Trend of Thermal Gradient During Standstill (Average Across Bearing Span). The Thermal Gradient Is Here Defined as the Difference Between the Average Temperature of Upper and Lower Half Shaft Sections.

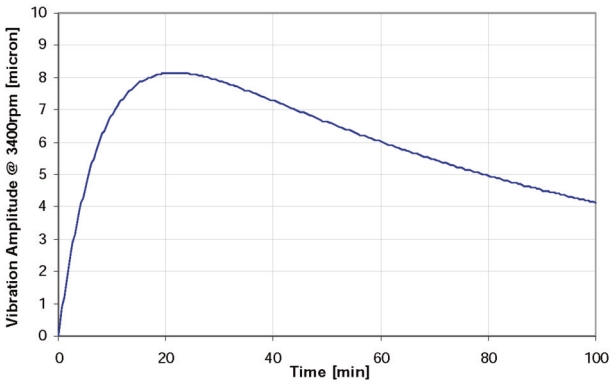

Figure 19. Predicted Vibration Amplitude During Slow Roll, Caused by Thermal Gradient Plotted in Figure 18.

IMPLICATIONS FOR THE END USER

The analytical model presented in the previous sections may be used to calculate the expected vibrations of a compressor during hot restart, but it requires a detailed knowledge of the thermodynamic and geometric parameters of the system and a quite lengthy calculation process, involving finite element analysis and rotordynamic analysis. Moreover, such a calculation does not provide general conclusions on compressor behavior during hot restart, since it refers to a single combination of operating parameters and boundary conditions.

During the design of a compressor, it would be more useful to quickly verify its sensitivity to rotor bow during hot restart and to compare it to existing references. In order to do this, the analytical model has been used to derive a single numerical parameter that is a combination of data available at an early stage of design, and that is proportional to the effect of hot restart on rotor vibrations. This activity is currently in progress; a parameter, called hot restart sensitivity (HRS) has been calculated and then tuned by comparing it to the available experimental data from a set of references. It encompasses the following factors:

- The thermal gradient ΔT that may develop across the rotor section
- The bowing of the rotor due to thermal gradient (displacement between bearing axis and rotor center of gravity)
- The time constant τ of the phenomenon

The formulation found for HRS is the following:

$$ND\left[L(T_{disch} - T_{suct})\right]^2 \sqrt{(p_{disch} + p_{suct})} \qquad (15)$$

where N is the MCS of the rotor, D and L are its impeller bore diameter and bearing span, respectively, and temperature and pressure refer to inlet and exit flange of the compressor.

Some physical interpretation is quite intuitive: hot restart is more critical for rotors that are large (high D) and flexible (high L and N), and for high thermal gradients developing during standstill (mainly due to high $T_{disch} - T_{suct}$ and to a lesser extent by gas thermal conductivity, that increases with gas pressure).

For internal use and for comparison with existing references and criteria, it was deemed useful to extract the shaft diameter D from the previous formula, and to put it on the x-axis of a diagram, reporting on the y-axis the parameter HRS expressed in the final formula below:

$$\mathrm{HRS} = N\left[L(T_{disch} - T_{suct})\right]^2 \sqrt{(p_{disch} + p_{suct})} \qquad (16)$$

The diagram is presented in Figure 20; parameters on x and y axes are normalized to 1. Comparison with experimental data and calculation results allow the conclusion that compressors outside the rectangular boundary shown on the diagram may be considered sensitive to hot restart.

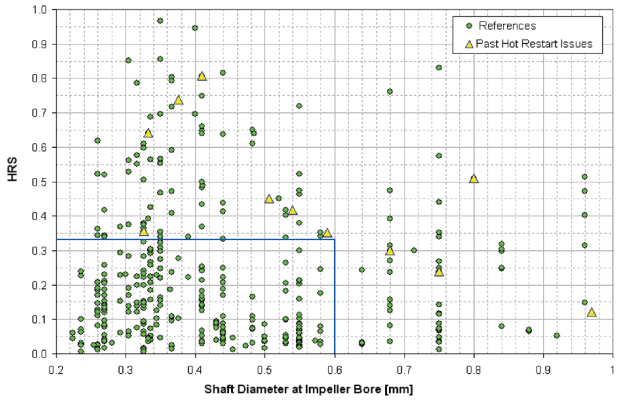

Figure 20. Reference Diagram Plotting Hot Restart Sensitivity Parameter Versus Shaft Diameter.

A modified formulation of HRS is in study for back-to-back compressors; nonetheless in first approximation Equation (15) may still be used, considering the following values:

- p_{suct} = Inlet pressure of the first section
- p_{disch} = Discharge pressure of the second section
- T_{suct} = Lowest suction temperature between first and second section
- T_{disch} = Highest discharge temperature between first and second section

If during the design phase a compressor is identified as highly sensitive to hot restart, the implementation of slow roll may be considered in order to mitigate the phenomenon. Alternatively, vibration issues may be avoided by restarting the compressor only after a standstill time sufficiently long to eliminate the rotor bow.

The speed that can be used for slow roll is constrained by the minimum speed required for dry gas seal liftoff (lower limit) and by the peak in compressor vibration amplitude corresponding to its first critical speed (upper limit; the required separation margin from first critical speed may be calculated in function of its amplification factor, as per API 617, 2002). In addition, other limitations due to the equipment connected to the compressor shall be considered (e.g., critical speeds of the driver).

The optimum duration for the slow roll speed is function of rotor size and slow roll speed; it may be tuned by performing hot restart tests similar to that shown in Figures 15, 16, 17.

As a final consideration, it should be noted that if alarm/trip levels for high radial vibrations are properly set, compressor damage during hot restart should be prevented independently from its sensitivity to the phenomenon. One possible exception is represented by compressors driven by fixed-speed electric motor, whose startup ramp can be so quick to reach.

CONCLUSION

An analytical model was developed in order to predict compressor vibrations due to hot restart. The model was applied to a real centrifugal compressor for which experimental data were available, and calculation results proved to be in good agreement with measured vibrations. Additional hot restart tests were specifically carried out on another compressor and allowed to further validate the predictions of the calculation model.

In the present paper the analytical formulation of the phenomenon has been used to predict the behavior of existing compressors, but its potential application is wider: allowing a quantification of the influence of any single geometric or thermodynamic parameter on hot restart vibrations, it may be helpful for design optimization or at least for developing a rough classification of centrifugal compressors according to their sensitivity to hot restart.

NOMENCLATURE

α	= Gas thermal diffusivity (m^2/s)
β	= Volumetric thermal expansion coefficient ($°C^{-1}$)
θ	= Angular position along shaft section (rad). $\theta = 0$ at bottom (stagnation point).
λ	= Gas thermal conductivity (W/[m·K])
λ_r	= Rotor thermal conductivity (W/[m·K])
μ	= Gas dynamic viscosity (Pa·s)
ν	= Gas kinematic viscosity (m^2/s)
φ	= Adimensional heat transfer efficiency: $\varphi(\theta) = Nu_\theta/Nu_0$
C_p	= Heat capacity (J/K)
c_p	= Specific heat capacity (J/(kg·K))
D	= Cylinder diameter (mm)
DE	= Drive end (side of the rotor)
g	= Gravity acceleration (m/s^2)
Gr	= Grashof number
h	= Convective heat transfer coefficient ($W/(m^2·K)$)
N	= Compressor maximum continuous speed (rpm)
NDE	= Nondrive end (side of the rotor)
Nu	= Nusselt number
Pr	= Prandtl number
Q	= Energy transferred by heat (W)
r_G	= Radial displacement between bearing axis and center of gravity (mm).
t	= Time (s)
T	= Temperature (°C)
T_∞	= Asymptotic gas temperature (°C)
T_s	= Source temperature (°C)
U	= Rotor unbalance (g·mm)
W	= Rotor mass (kg)

REFERENCES

API Standard 617, 2002, "Axial and Centrifugal Compressors and Expander-Compressors for Petroleum, Chemical and Gas Industry Services," Seventh Edition, American Petroleum Institute, Washington, D.C.

Çengel, Y. A., 2003, Heat Transfer: a Practical Approach, New York, New York: McGraw Hill Professional.

Oertel, H. (editor), 2004, Prandtl's Essentials of Fluid Mechanics, New York, New York: Springer-Verlag New York Inc.

BIBLIOGRAPHY

Muszynska, A., 2005, *Rotordynamics*, Boca Raton, Florida: CRC Press.

Young, W. C. and Budynas, R. G, 2002, *Roark's Formulas for Stress and Strain (7th Edition)*, New York, New York: McGraw Hill Professional.